

# Lenacapavir impurity analysis

Qingsong Wang<sup>1</sup>, Yongfeng Qiu<sup>2</sup>

<sup>1</sup>Wisdom Pharmaceutical co.,LTD. Haimen 226123, Jiangsu, China

<sup>2</sup>School of pharmaceutical sciences, Fudan university, Shanghai 201203, China

**Copyright:** © 2025 Author(s). This is an open-access article distributed under the terms of the Creative Commons Attribution License (CC BY 4.0), permitting distribution and reproduction in any medium, provided the original work is cited.

**Abstract:** On June 20, 2024, Gilead Sciences announced the interim results of the pivotal Phase 3 PURPOSE 1 trial for Lenacapavir, a new HIV prevention drug administered via subcutaneous injection twice a year, demonstrating 100% efficacy in preventing HIV infection in young women.

On August 22, 2022, the European Commission approved Lenacapavir globally for use in combination with other antiretroviral drugs to treat adult HIV-infected patients with multidrug-resistant virus who cannot achieve viral suppression.

The synthesis of the key intermediate LNKPW01 for Linaclootide involves the Suzuki reaction, during which we identified several impurities. Through in-depth investigation of these impurities, we gained a deeper understanding of the process. Let's take a closer look at these impurities, with impurity M being the most significant.

**Keywords:** Lenvatinib; Process; Impurities

**Online publication:** December 26, 2025

## 1. Synthesis of LNKPW01

The synthesis route and process are as follows:

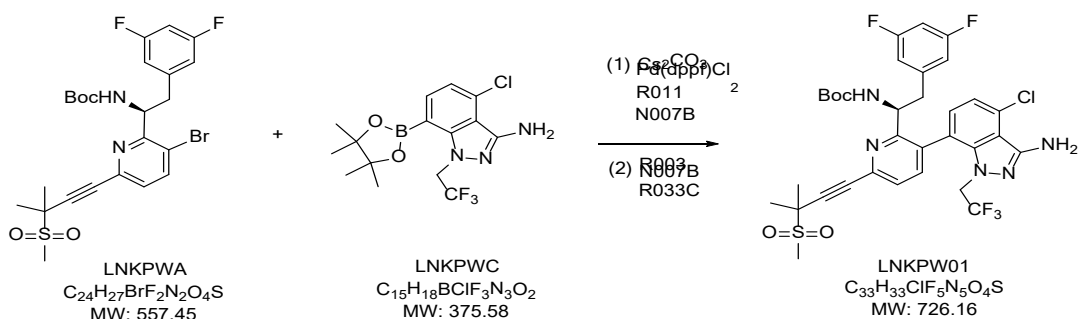


Figure 1. The synthesis route and process LNKPW01

Synthesis process: 1.0eq LNKPWA, 1.2eq LNKPWC, 1.5eq Cs<sub>2</sub>CO<sub>3</sub>, 10.0V/W THF, 2.0V/W N007B, N<sub>2</sub> displacement three times, add 0.05eq Pd (dppf) Cl<sub>2</sub>, N<sub>2</sub> displacement three times, heat up to 80°C for 4 hours, TLC control LNKPWA reaction is complete, the reaction solution is dissolved to dryness, 5.0V/W EA is added, and after dissolution,

it is washed twice with 2 \* 2.0V/W H<sub>2</sub>O. After organic addition to MTBE, a solid is precipitated and filtered to obtain LNKPW01 product. The purity of the obtained LNKPW01 product is only 75-85%.

## 2. The HPLC chromatogram of the reaction solution is as follows

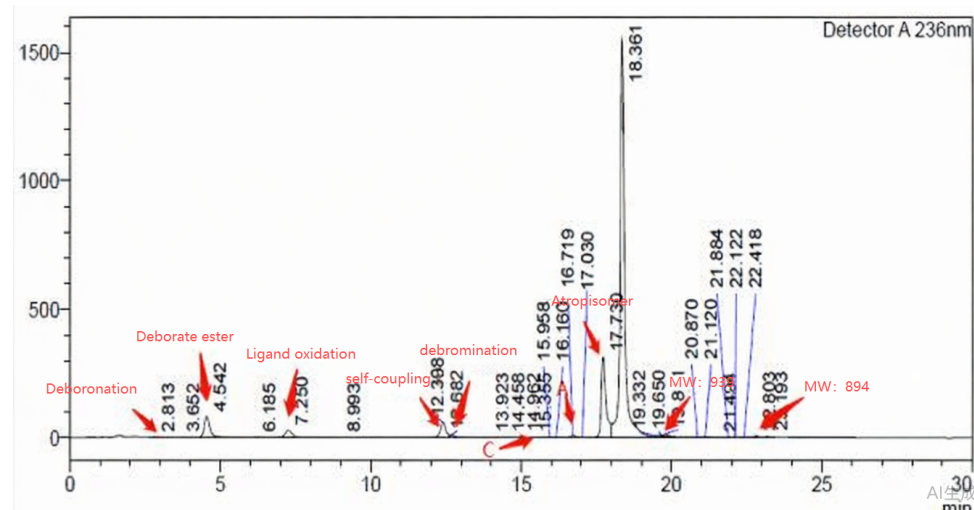


Figure 2. The HPLC chromatogram of the reaction solution

As shown in the above figure, the main impurities involved in the reaction include C dehydroborylation products, C dehydroborate ester products, ligand oxidation products, C self coupling products, debromination products, hindered isomers, impurities with a molecular weight of 939, and impurities with a molecular weight of 894.

## 3. Impurity analysis of reaction solution

### 3.1. Boron deprotonation products

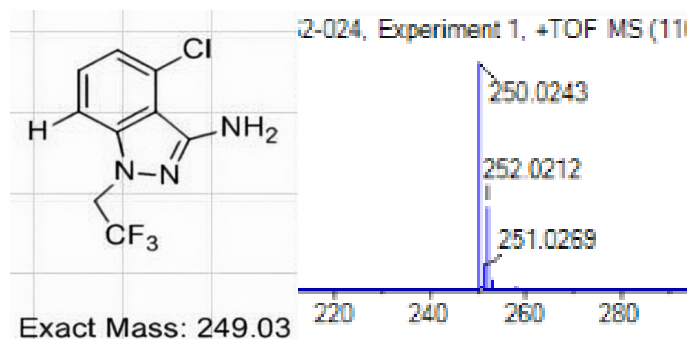


Figure 3. The LCMS spectrum and analytical structural formula of the impurity

The LCMS spectrum and analytical structural formula of the impurity are shown in the figure above<sup>[1]</sup>. The impurity accounts for about 5% of the reaction solution. Borination is a common impurity in Suzuki coupling reactions, which can occur under the action of water, acid, and base. Under alkaline conditions, boric acid forms an unstable adduct with hydroxide ions, and after a transition state, boric acid is removed to produce protonated products. The deprotonation mechanism of boronic acid esters under alkaline conditions is relatively complex, mainly involving two pathways<sup>[2]</sup>. Firstly, the hydroxyl adducts of boronic acid esters can be directly deprotonated. Another approach is to first hydrolyze the

boronic acid ester adduct into a boronic acid adduct, and then proceed with boron removal<sup>[3]</sup>.

### 3.2. Dehydration products of boron (oxidation products)

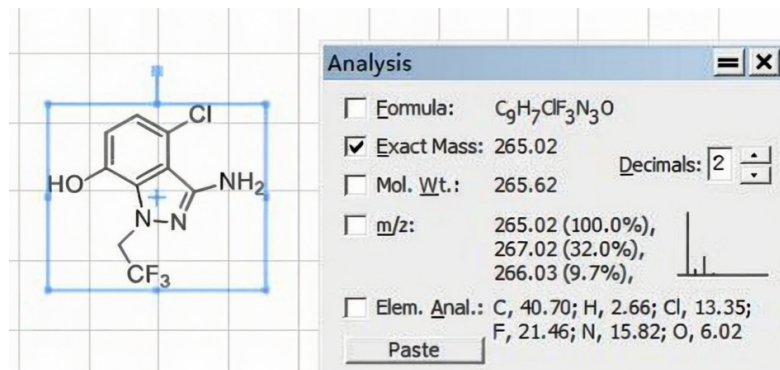


Figure 4. LCMS and structural analysis of the trace impurity (~0.15% by TOF) in the deborylative hydroxylation product.

The LCMS spectrum and analytical structural formula of the impurity in the boron removal hydroxylation product are shown in the figure above. The Suzuki coupling reaction produces boron removal hydroxylation products in the presence of oxygen<sup>[4]</sup>. Compared with the boron removal protonation products, the boron removal hydroxylation products are only trace amounts, but the impurity was indeed detected on TOF at about 0.15%.

### 3.3. Ligand oxidation products

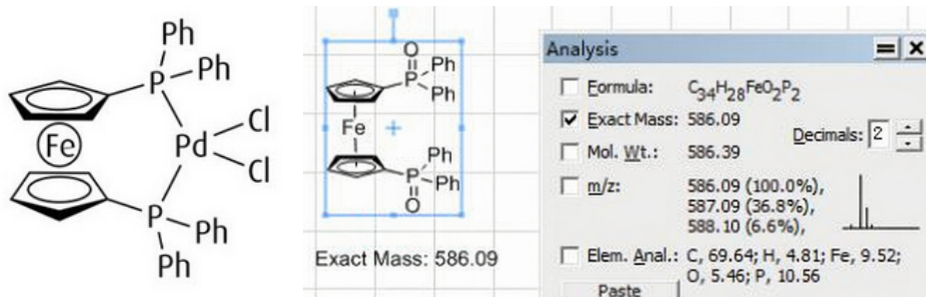


Figure 5. LCMS spectrum and analytical structural formula of the impurities

The catalyst [1,1 '- bis (diphenylphosphine) ferrocene] palladium dichloride will be oxidized in the presence of oxygen, producing oxidation impurities, which account for about 2% of the reaction solution. The LCMS spectrum and analytical structural formula of the impurities are shown in the above figure<sup>[5]</sup>.

### 3.4. Boric acid (ester) dehalogenation self coupling product

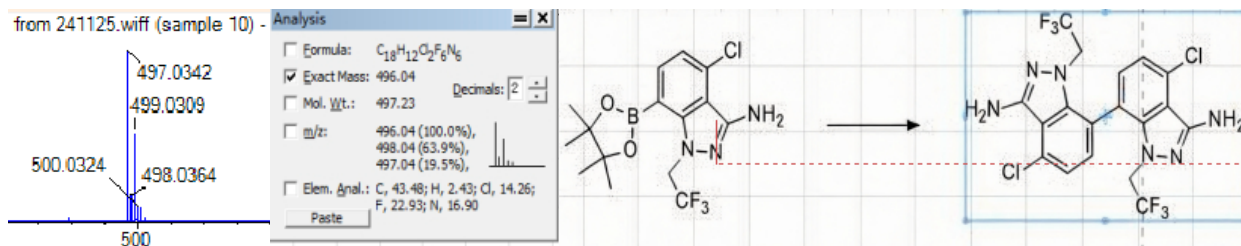


Figure 6. The LCMS spectrum and analytical structural formula of boronic acid (ester) dehoronation self coupling products

The LCMS spectrum and analytical structural formula of boronic acid (ester) dehoronation self coupling products are shown in the figure above<sup>[6]</sup>. In 2006, based on previous research, Carlo Adamo et al<sup>[7,8]</sup> further improved the mechanism of boronic acid self coupling through detailed control experiments, kinetic studies, and DFT (Density Functional Theory) calculations, and proposed a more detailed mechanism. This mechanism highlights the roles of oxygen, boric acid, and water at different stages throughout the catalytic process. The mechanism is as follows:

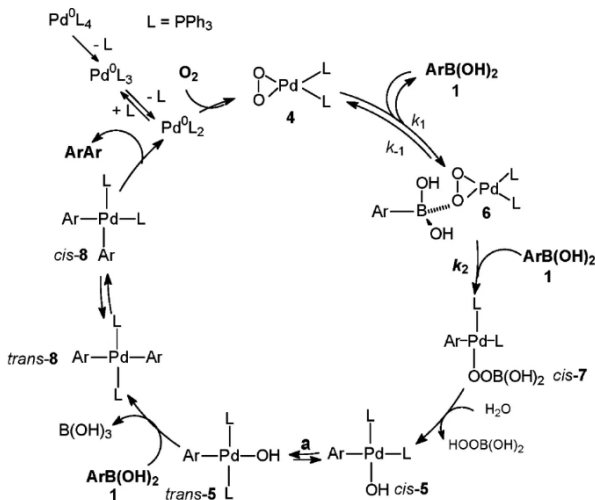


Figure 7. the mechanism of boronic acid self coupling

1. Zero valent Pd (0) is first oxidized by oxygen to form ternary active Pd species 4<sup>[9]</sup>
2. 4 reacts with one molecule of boric acid to generate 6
3. 6. Transfer metalization occurs with another molecule of boric acid to generate intermediate cis-7
4. CIS-7 reacts with water to generate CIS-5
5. Cis-5 isomerizes to trans-5, which is the reactive intermediate
6. Trans-5 undergoes transfer metalization with the third molecule boric acid to generate the intermediate trans-8
7. Trans-8 also undergoes isomerization to generate cis-8
8. 9 undergoes reduction and elimination, generating self coupling products.

### 3.5. Dehalogenation impurities

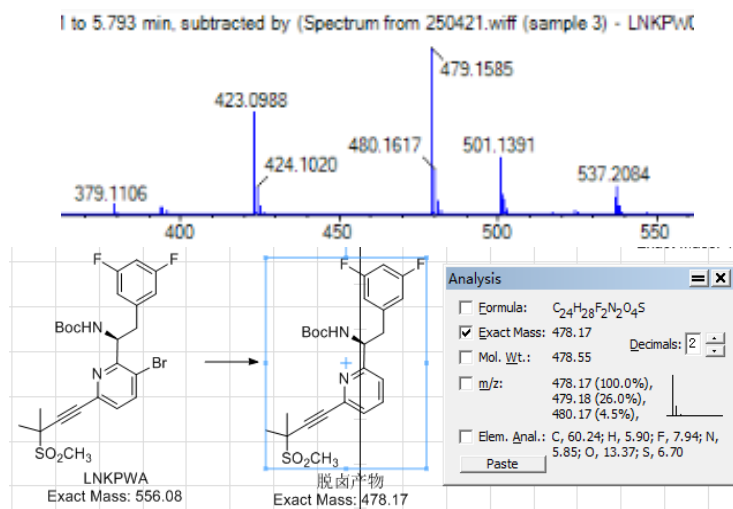


Figure 8. The LCMS spectrum and analytical structural formula of dehalogenation impurities

The LCMS spectrum and analytical structural formula of dehalogenation impurities are shown in the above figure, and the classical mechanism of dehalogenation is shown in the following figure<sup>[4]</sup>:

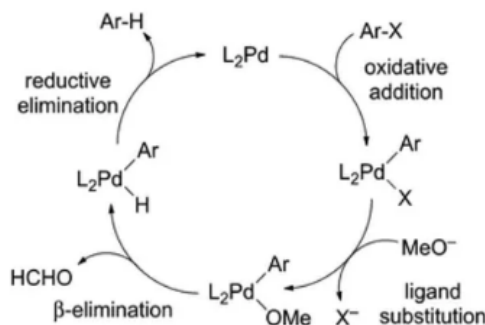


Figure 9. the classical mechanism of dehalogenation

The main process of this mechanism includes:

1. Oxidative addition of halogenated hydrocarbons to Pd (0) complexes
2. Substitution of halogen ions in complexes by alkaline centers<sup>[10]</sup>
3. The complex undergoes  $\beta$  - elimination to generate corresponding aldehydes, ketones, and palladium hydrides<sup>[11]</sup>
4. Reduction and elimination of palladium hydride to produce dehalogenated products<sup>[12]</sup>
5. The core viewpoint of this mechanism is that oxidative addition is the rate limiting step, and the addition of base and catalyst is necessary for dehalogenation. The increase of base often leads to an increase in dehalogenation products<sup>[13]</sup>.

### 3.6. Tandem side reaction impurities (Mw=894 and Mw=938)

Two impurities were found behind the main peak, with impurities with a molecular weight of 938 accounting for approximately 0.4-0.5% and impurities with a molecular weight of 894 accounting for approximately 2%. When the reaction is incomplete and boronic acid ester C is added, these two impurities will increase. The TOF results are as follows:

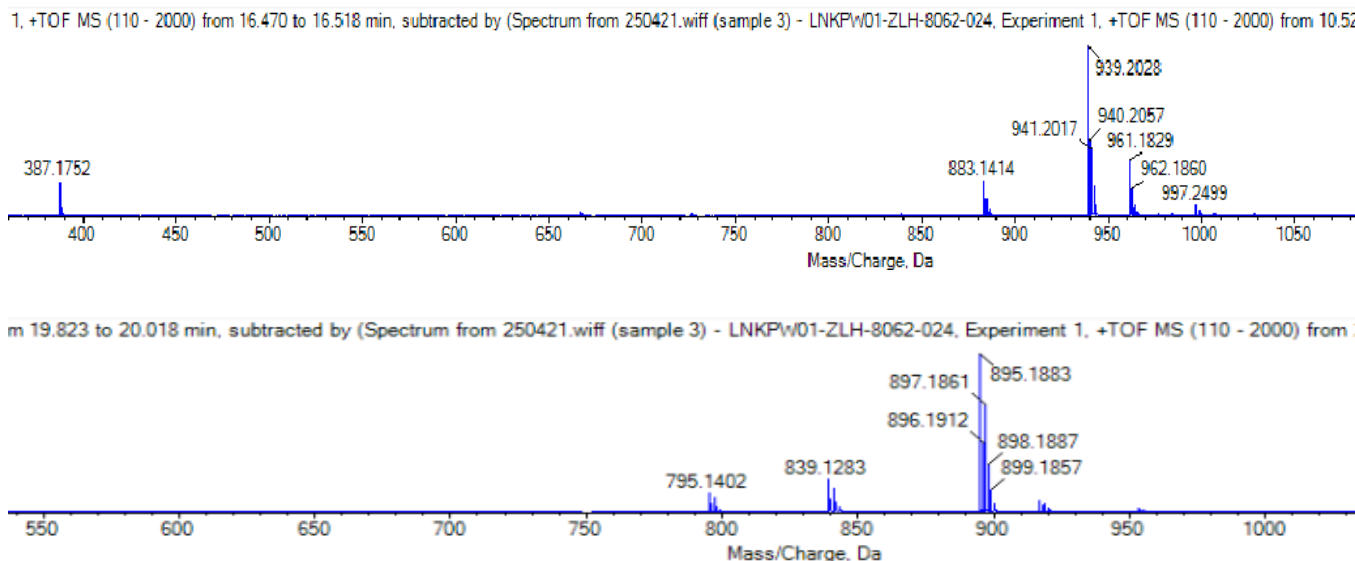
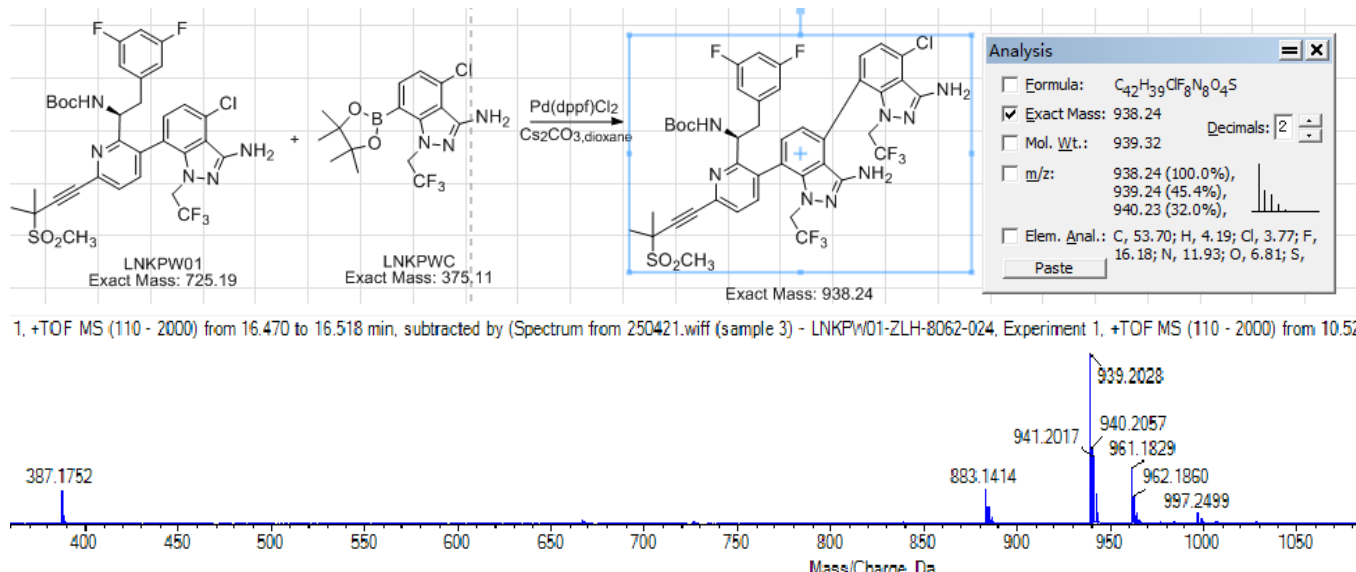
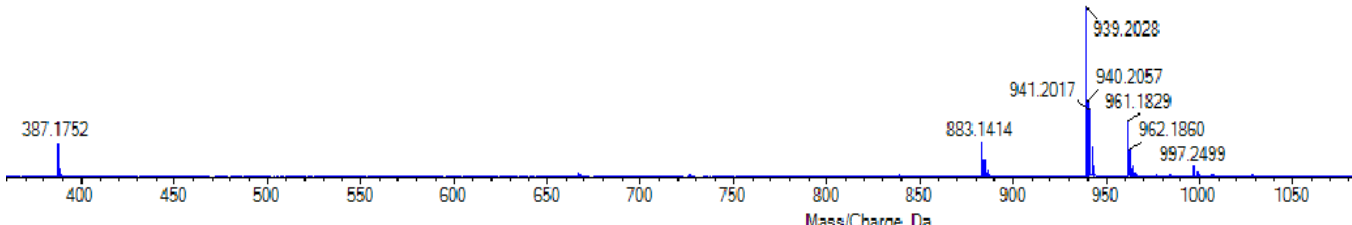


Figure 10. TOF analysis of M\_w 894 (~2%) and M\_w 938 (~0.5%) impurities

### 3.6.1. Serial side reaction impurities ( Mw=938 )



1. +TOF MS (110 - 2000) from 16.470 to 16.518 min, subtracted by (Spectrum from 250421.wiff (sample 3) - LNKPW01-ZLH-8062-024, Experiment 1. +TOF MS (110 - 2000) from 10.52



**Figure 11.** The LCMS spectrum and analytical structural formula of the impurity (Mw=938) in the series side reaction

The LCMS spectrum and analytical structural formula of the impurity (Mw=938) in the series side reaction are shown in the above figure, and the peak of 939 is M+1; The peak of 961 is 938+23; The peak of 883 is 939-56.

### 3.6.2. Tandem side reaction impurities (Mw=894)

m 19.823 to 20.018 min, subtracted by (Spectrum from 250421.wiff (sample 3) - LNKPW01-ZLH-8062-024, Experiment 1. +TOF MS (110 - 2000) from

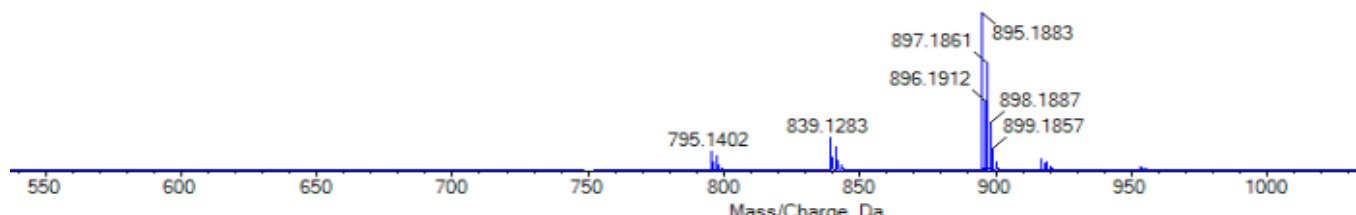


**Figure 12.** The LCMS spectrum of the impurities (Mw=894) in the series side reaction

The LCMS spectrum of the impurities (Mw=894) in the series side reaction is as shown above, and the initial speculated structure is as follows:

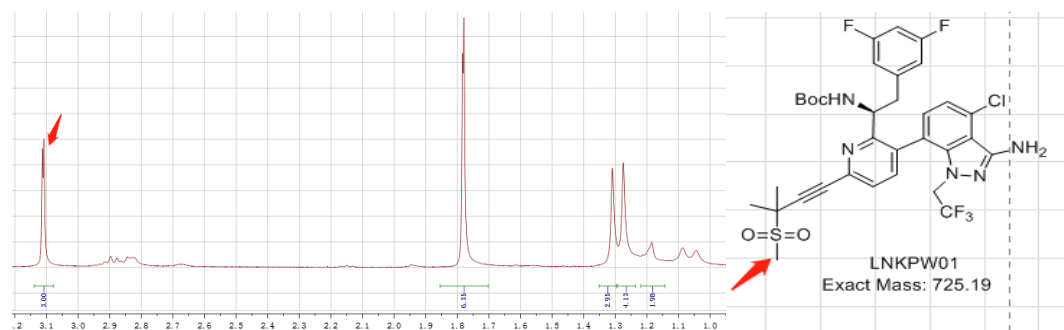


**Figure 13.** the initial speculated structure

The H-NMR of LNKPW01 is as follows:

The H-NMR of impurity (Mw=894) is as follows:

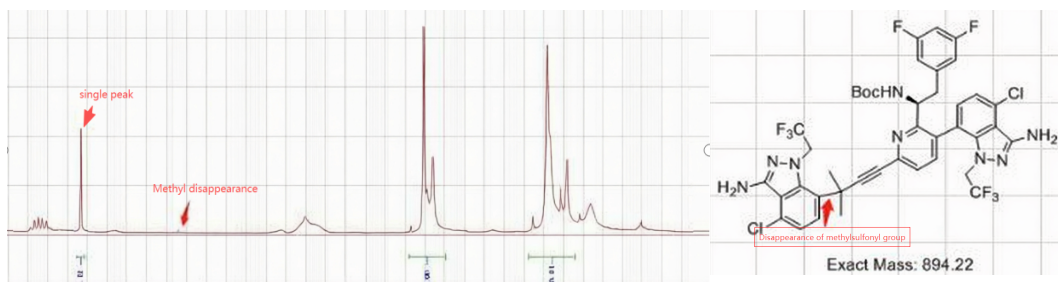


Figure 14. The H-NMR of LNKPW01 and The H-NMR of impurity

By comparison, it can be found that the methylsulfonyl group of LNKPW01 exhibits a single peak with an integral of 3 at position 3.1, but there is no peak at position 3.1 in the NMR hydrogen spectrum of the impurity (Mw=894), indicating that the methylsulfonyl group has indeed been lost. Further compare the hydrogen spectrum of LNKPW01 with the hydrogen spectrum of impurity (Mw=894).

LNKPW01 low field hydrogen nuclear magnetic resonance analysis:

Mw=894 impurity low field H-NMR analysis:

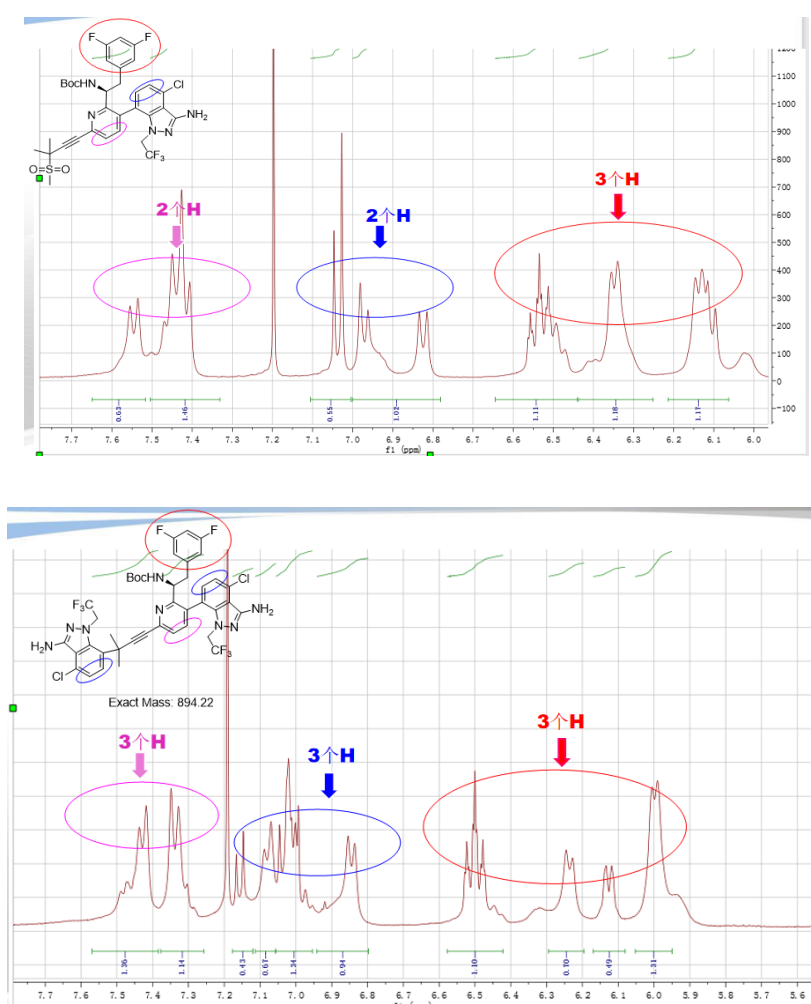
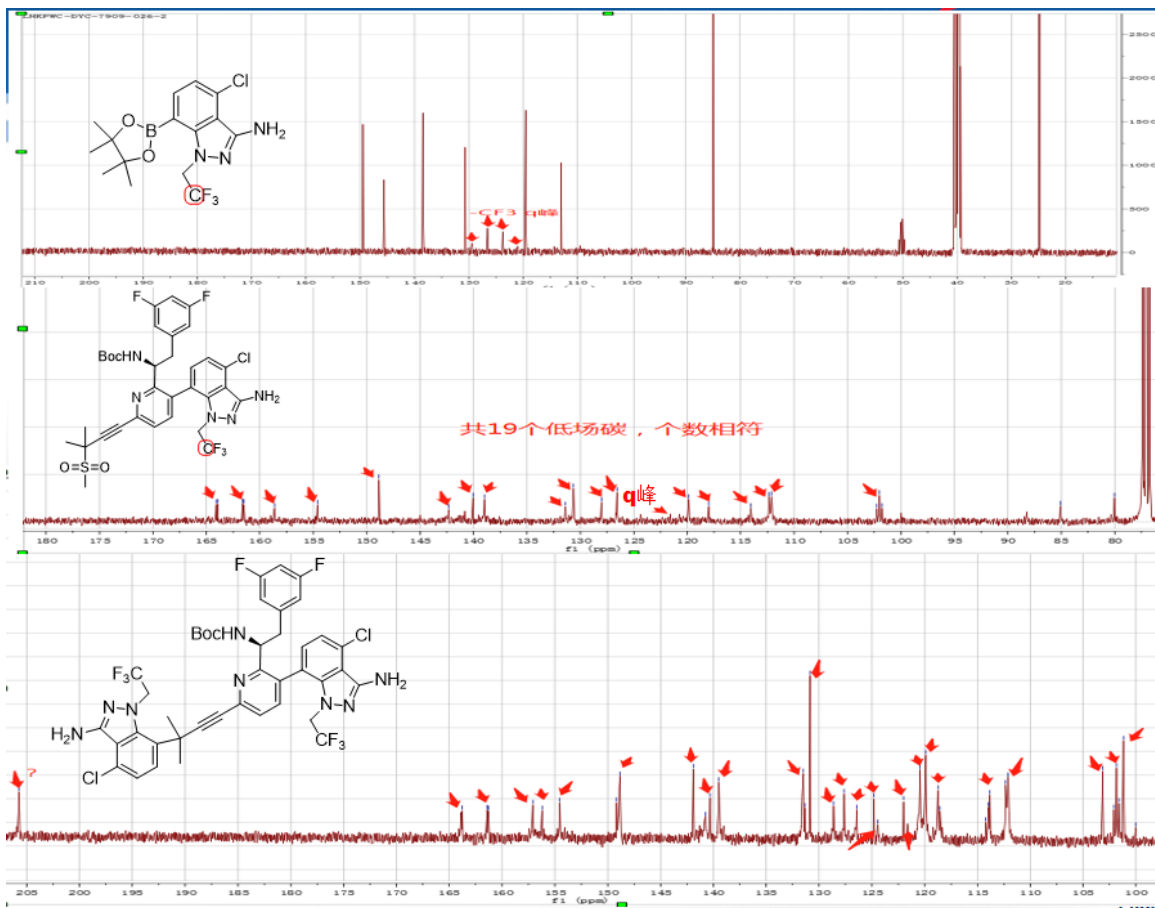


Figure 15. LNKPW01 low field hydrogen nuclear magnetic resonance analysis

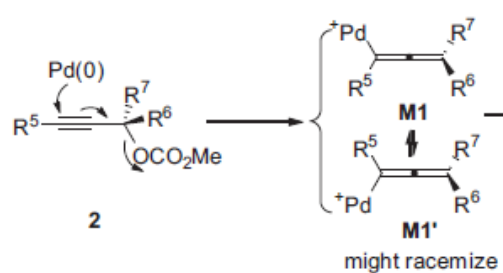
**Figure 16.** Mw=894 impurity low field H-NMR analysis

By comparing the LNKPW01 H-NMR with the low field H-NMR analysis of 894 impurity, it was found that the H-NMR Mw-894 impurity is also basically consistent. Below is an analysis of the C-NMR of impurity 894:

**Figure 17.** analysis of the C-NMR of impurity 894

The carbon spectrum and speculated structure of impurity 894 are also basically consistent, but a single peak appears around 207, which does not match the speculated structure.

Through literature review, it was found that olefins can transform into dienes under palladium carbon catalysis. The mechanism described in the literature is as follows<sup>[14]</sup>:

**Figure 18.** The mechanism described in the literature

Based on the literature, we speculate that the impurity structure and mechanism of 894 should be as follows:

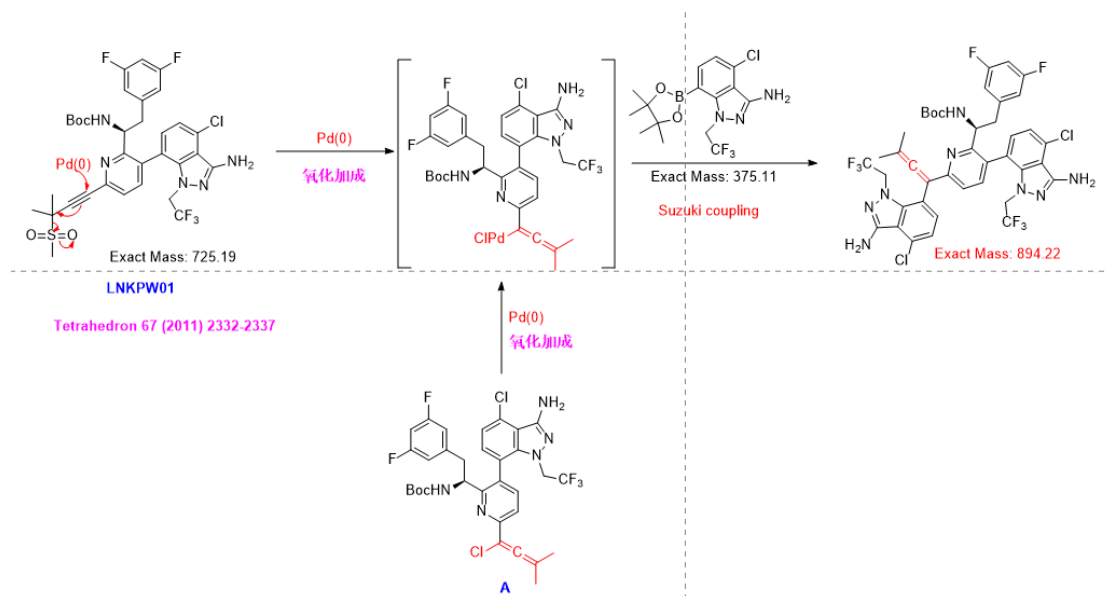


Figure 18. the impurity structure and mechanism of 894

## Reason:

1. The isotopic peak of chlorine shows a ratio of 9:6:1, which is consistent with two chlorides;
2. The methyl group of the methylsulfonyl group disappears in both the hydrogen and carbon spectra, consistent with the Mestrenova simulation;
3. The number and position of hydrogen and carbon spectra are consistent, and the carbon position of the diene is exactly around 2.5.

## Disclosure statement

The author declares no conflict of interest.

## References

- [1] Emmons W D, 1961, Peroxides. IV. Polypeoxides. J. Am. Chem. Soc, 83(7): 1733–1738.
- [2] Bothner-By A A, Foote C S, 1961, Rates of Reaction of Diphenylpicrylhydrazyl with Phenols and Amines. J. Am. Chem. Soc, 83(10): 2164–2166.
- [3] Toyoda K, Tashiro S, Takeuchi MT, 2021, Discovery of a Peptide Nucleation Factor for Digestive Organelle Formation. J. Am. Chem. Soc, 143(7): 2818–2827.
- [4] Hoffmann H M R, Heiermann K E K, 1978, Reaction of  $\alpha,\beta$ -Unsaturated Carbonyl Compounds with Diazoalkanes. J. Org. Chem, 43(8): 1619–1620.
- [5] Li W, Wang Y, Wang Z A, 2014, Continuous Process for the Production of  $\gamma$ -Butyrolactone. Org. Process Res. Dev, 18(3): 501–510.
- [6] Grissom J W, Klingberg D, 1996, Tandem Radical Cyclization-Rearrangement Reactions. J. Org. Chem, 61(7): 2346–2351.
- [7] Grieco P A, Henry K J, 2003, An Efficient Synthesis of cis-2,5-Disubstituted Pyrrolidines. Tetrahedron Lett, 44(9): 154–1544.
- [8] Zhang W, Curran D P, 2006, Synthesis of Fluorous Oxazolidinones and Their Use in Enantioselective Aldol Reactions. J.

Am. Chem. Soc,128(21): 6829–6836.

- [9] Shi F, Tse M K, 2009, Copper-Catalyzed Enantioselective Henry Reaction. *Angew. Chem., Int. Ed* ,48(32): 5912–5915.
- [10] Zhu W, Mena M, Noël S, 2011, Synthesis of 2-Amino-3-cyano-4H-chromenes. *Tetrahedron* ,67(12): 2332–2337.
- [11] Ragan J A, am Ende D J, Hill P D, 2007, Development of a Safe and Scalable Process for a Key Intermediate. *Org. Process Res. Dev*,11(5): 799–805.
- [12] Wu Z, Yu J, Wu J, 2020, Continuous-Flow Synthesis of a Pharmaceutical Intermediate. *Org. Process Res. Dev*, 24(2): 228–234.
- [13] Bryan M C, Dunn P J, 2018, Key Green Chemistry Research Areas from a Pharmaceutical Perspective. *Org. Process Res. Dev*, 22(4): 542–584.
- [14] Ma S, Gu Z, 2006, Palladium-Catalyzed Cyclization of 1,3-Dienes. *Chem. Commun*, (1): 94–96.

**Publisher's note**

*Whioce Publishing remains neutral with regard to jurisdictional claims in published maps and institutional affiliations.*